A R A, inc.

AEROSPACE RESEARCH ASSOCIATES

2017 WEST GARVEY AVENUE   •   WEST COVINA, CALIFORNIA   •   TEL. 962-1045

Second Quarterly Progress Report

on

"Concepts of Multiple-Impact Study

of Energy Absorption"

ARA Report
#26

14 October 1963

Reporting Period: 1 July 1963 - 1 October 1963

Contract Number: NAS 7-226

Technical Status Report #2

Prepared by:

Dr. David L. Platus, Project Scientist

Patrick J. Cunningham, Project Engineer

Frank A. Marovich, Engineer

Holland H. Freeman, Engineer

Approved by:

Bernard Mazelsky, President, ARA, Inc.

TABLE OF CONTENTS

iii

LIST OF FIGURES AND TABLES

SECOND QUARTERLY PROGRESS REPORT
ON
"CONCEPTS OF MULTIPLE-IMPACT STUDY OF ENERGY ABSORPTION"

25770

I. SUMMARY

Cyclic torsional testing apparatus for studying materials in relation to cyclic strain energy impact devices is described. The apparatus provides cyclic stress-strain curves for materials under conditions representative of those occurring under impact cycling conditions. Calibration procedures and data reduction methods are described and the results of preliminary runs on aluminum are presented.

The results of a brief study of cyclic strain energy devices in relation to crew protection applications is presented, and several key problem areas are identified. The design of a "torus" impact device, applicable to crew protection systems, is described.

II. INTRODUCTION

This report summarizes work carried out during the second quarter under NASA Contract NAS 7-226, "Concepts of Multiple-Impact Study of Energy Absorption." The major effort has been concerned with (1) assembly, modification, and calibration of the cyclic torsion testing apparatus, and development of procedures for data reduction; (2) preliminary testing of several aluminum samples; (3) a brief study of cyclic strain energy devices in relation to crew protection applications; and (4) design of a "torus" impact device to be tested in a later phase of the experimental program.

In a previous report (Ref. A), relations between the performance of cyclic strain energy devices and the flow and fatigue characteristics of the working metal were developed. It was shown that load-stroke behavior of these devices could be directly related to the behavior of the hysteresis loop during cyclic straining and that the specific energy absorption (SEA) capability was related to the fatigue life as well. The cyclic torsional apparatus and testing procedures described in Section III represent part of an experimental program to study cyclic straining of materials under impact cycling conditions.

A second phase of the experimental program will be concerned with testing of a cyclic strain energy impact device. The basic material data developed in the first phase will be used with the previous analytical models to predict the performance of the device under actual impact conditions. In order to select a promising design with regard to space applications, a brief study of cyclic strain energy devices in relation to crew protection systems was conducted and is described in Section IV. Several problem areas were identified and given consideration in the selection of the device described in Section V.

III.   CYCLIC TORSION TESTING

    A.   Test Apparatus

        The cyclic torsion testing apparatus is schematically outlined in Figure 1 and a photo of the assembly ready for use (Figure 2) illustrates the mechanical-electrical layout of the mechanism.
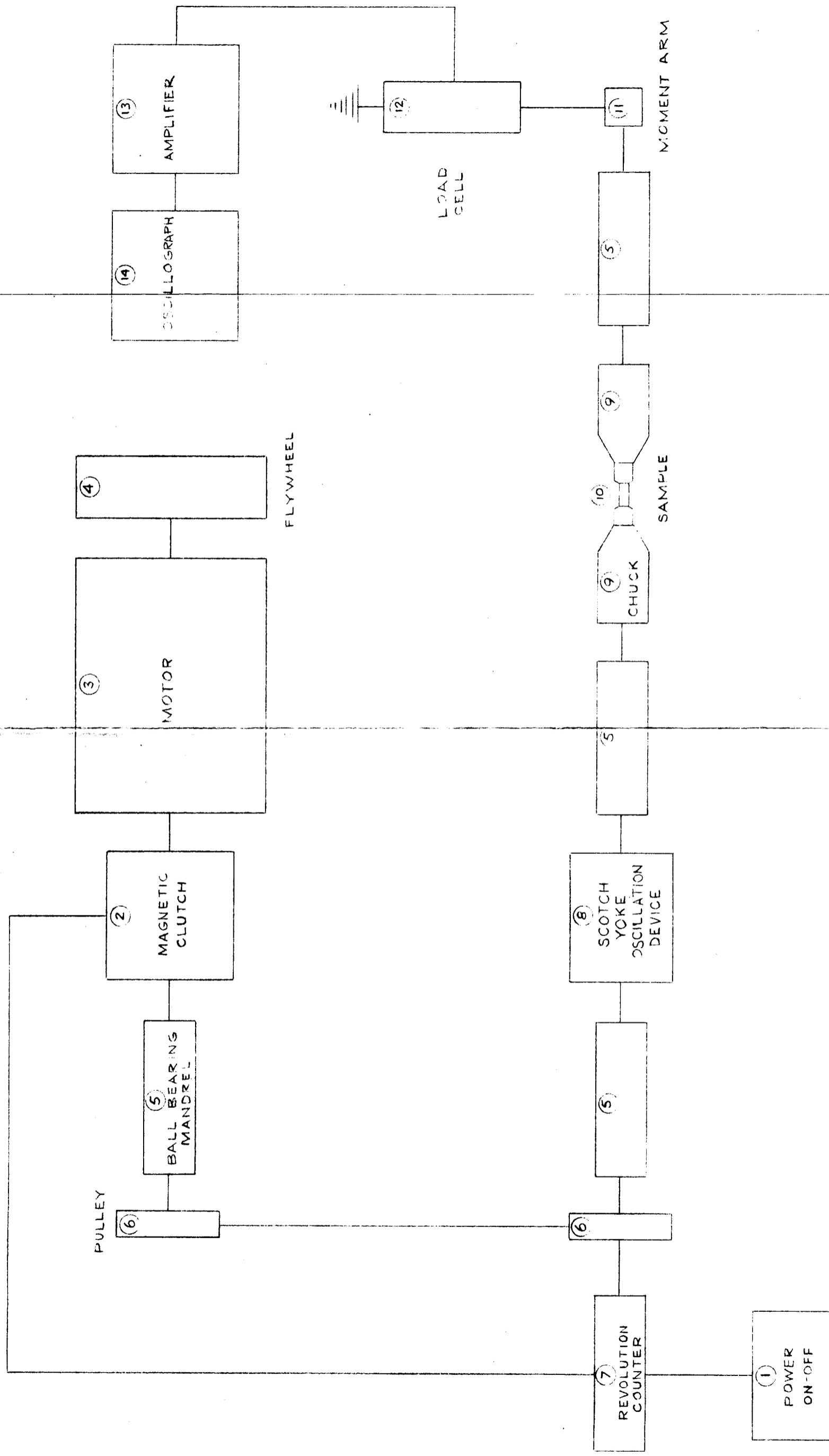
FIGURE 1. SCHEMATIC, CYCLIC TORSION TEST APPARATUS

(13) AMPLIFIER

(14) OSCILLOGRAPH

(12) LOAD CELL

(11) MOMENT ARM

(5)

(9)

(10)

(9) CHUCK

SAMPLE

(5)

(4) FLYWHEEL

(3) MOTOR

(2) MAGNETIC CLUTCH

(5) BALL BEARING MANDREL

(6) PULLEY

(6)

(8) SCOTCH YOKE OSCILLATION DEVICE

(5)

(7) REVOLUTION COUNTER

(1) POWER ON-OFF

Figure 2.
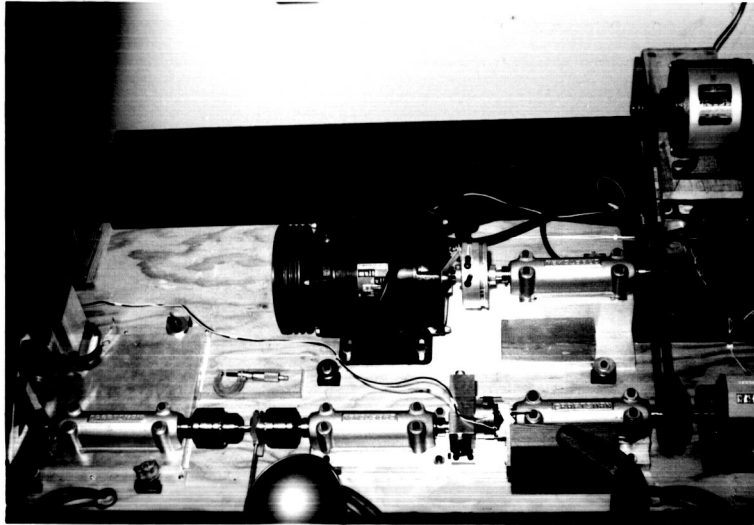
Assembly of Cyclic Strain Apparatus
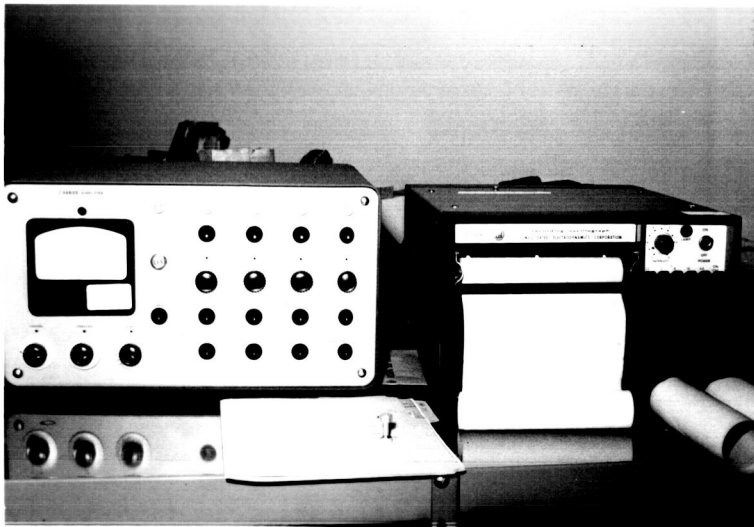
Amplifier and Oscillograph

Assembly of the mechanical parts was accomplished without difficulty and electrical matching of the transducer to the amplifier for the correct oscillographic record only required the selection of a new galvanometer. The previously selected galvanometers did not perform at the proper sensitivity range required for the torsion forces and frequencies that the amplifier was designed to control. Of the two galvanometers selected for the tests, one was too sensitive and the other was not sensitive at the lowest torques.

Careful testing of the apparatus with special test devices and actual specimens at all the expected test conditions revealed the following problem areas: a time signal was required to relate strain to its original zero position with respect to the input shaft rotation; a lock was required to restrain the moving chuck at high frequencies; a mechanical bias adjustment was required to prevent a zero shift of the transducer during the setup operation; a pointer was required to permit calibration of elastic deflections of the system at various torques in order to determine the actual specimen strain range.

A calibration of the system was performed to provide reference data for the actual specimen tests. The checkout testing determined the torque ranges required for calibration data. The transducer output versus input plus and minus torque was calibrated by means of level beam and dead weights (Figure 3). In addition to the output calibration, a deflection versus torque calibration of the transducer was performed in order to determine the actual strain amplitude at load. Various other deflections were measured for reference.

Figure 3.
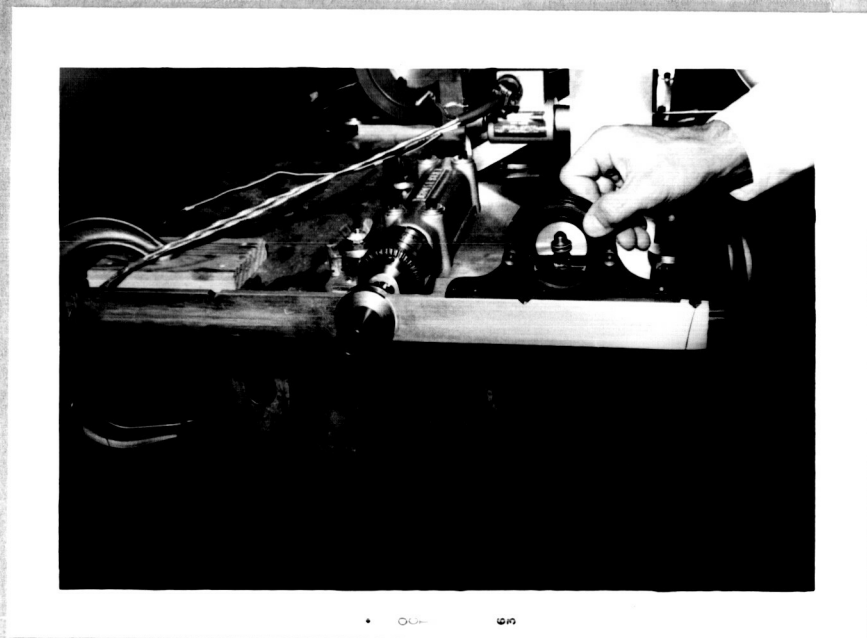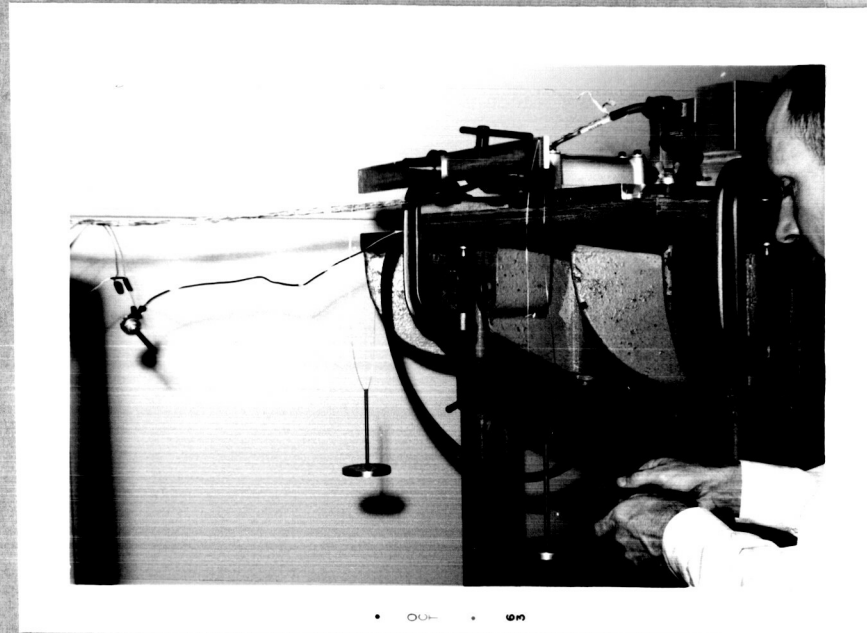
Dead Weight Calibration of Transducer

A pulse generator (Figure 4) was installed on the cam shaft in order to record the points of maximum strain input. The device consists of a galvanometer connected to a current source and is activated by the switch with rotation of the cam shaft.

B.   Test Procedure

The parameters of testing, i.e., cyclic rate, strain range, temperature, and total cycles, have been tabulated into a program that will require 12 specimens of each material for the initial room temperature tests. The cyclic rates are 1.5, 17.5, and 100 cycles per second. Total strain ranges are approximately .006, .012, .025, and .050 for the aluminum specimens. Each specimen is installed at zero torque and then one cycle of strain is hand cranked while measuring the strain amplitude (Figure 5) and maximum torque output. Then the sample is cycled approximately 20 times for records and visual observation (Figure 6). The sample is then cycled to failure and the total cycles are noted. Oscillograph records are made of the initial 20 cycles and periodically during the run to failure. A time pulse built into the oscillograph record provides an accurate time base to measure cyclic rate. The mean zero of the recorded wave form amplitude together with the pulse record provide the sine wave reference required to locate the theoretical input strain curve. By measuring the difference between the sinusoidal strain wave and the recorded wave form, a stress-strain curve may be plotted. This procedure is described more fully in the following section. The amplitude of the records indicate the torque and variations in amplitude during a run indicate the strain hardening effects.

Figure 4.
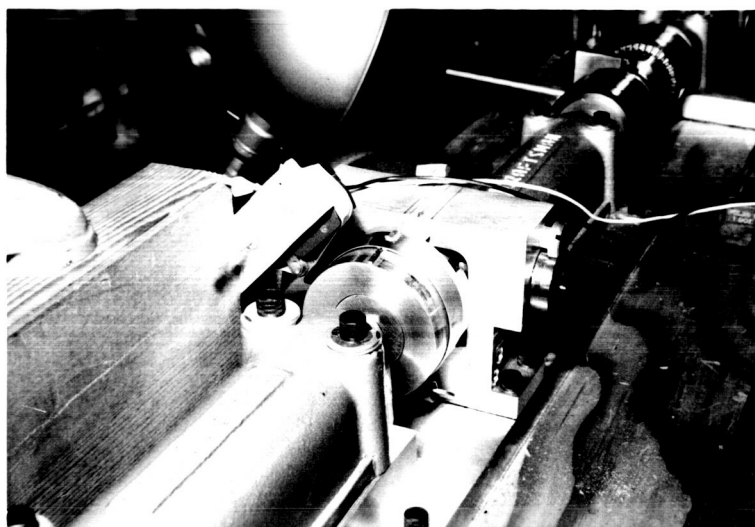
Pulse Generator on Input Cam Shaft

Figure 5.
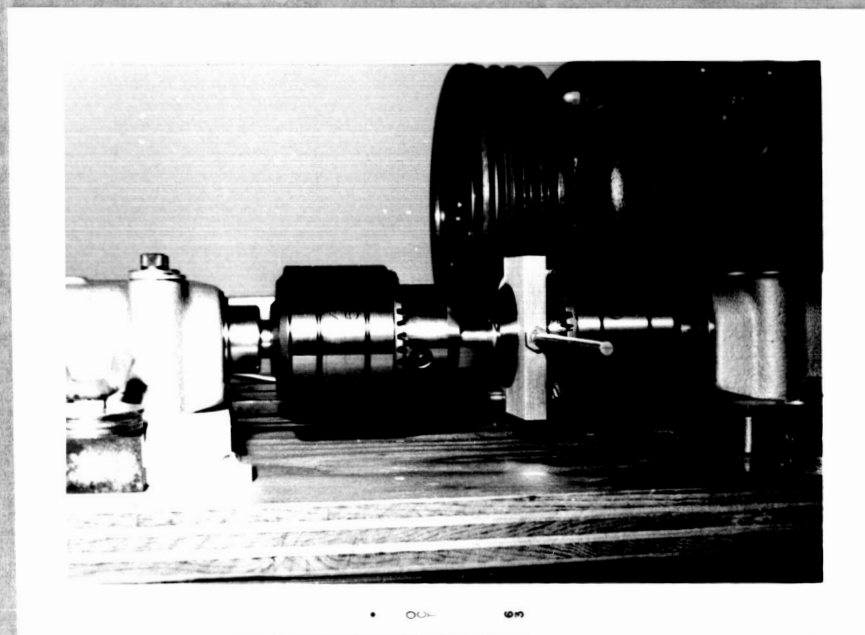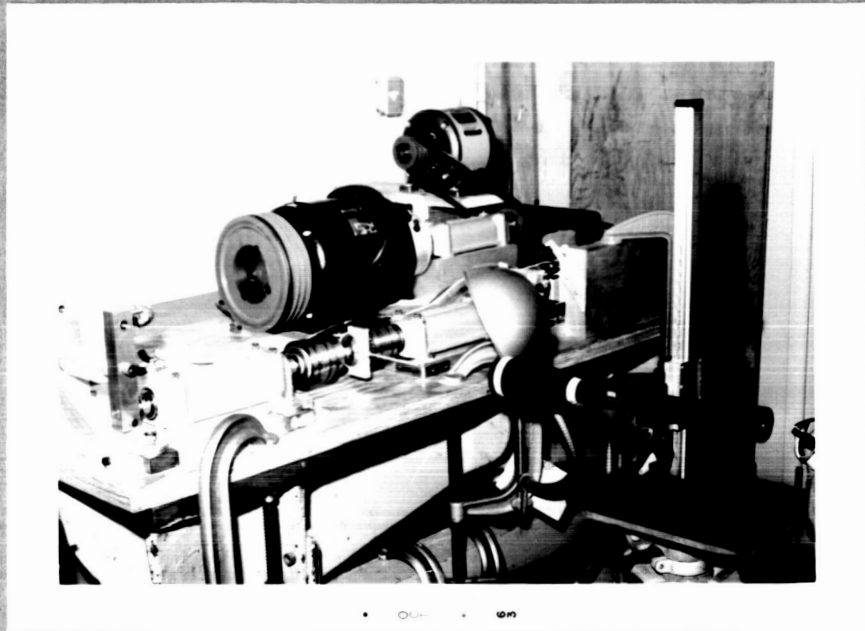
Measuring Telescope and Deflection Pointer

Figure 6.

Oscillograph Record and Aluminum Specimens

Several aluminum samples have been successfully tested. All the adjustments were found to be adequate and the electrical outputs have remained steady and repeatable. Some minor difficulty was experienced during the angular measurement phase due to the necessity of predicting the torque and therefore the overallowance to set in the initial deflection of the cam. Testing history demonstrates that this problem will be easily controlled.
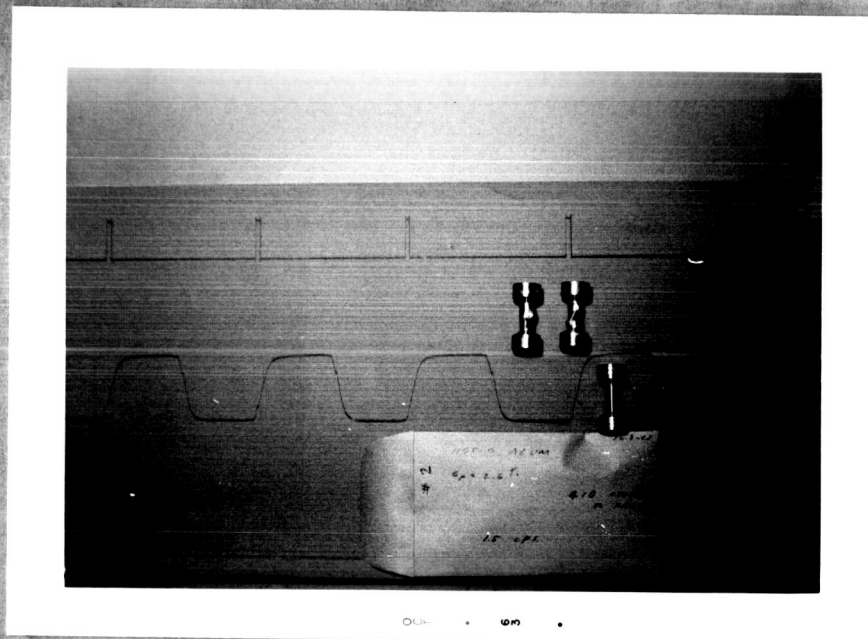
C. Data Reduction Procedure and Preliminary Results

The basic procedure for constructing a stress-strain curve consists of eliminating the time variable from the load-time record (Figure 6) and the approximate sinusoidal strain input. The period and phase of the strain curve are established with the aid of the time pulses on the oscillograph records, described above. Corrections must be applied to the sinusoidal input at the cam in order to account for the elastic deflections in the system. This is accomplished with the aid of the static torque-deflection calibration curves. For each value of torque read off the load-time record, the corresponding wind-up of the shafts is subtracted from the sinusoidal input to give the true deflection of the specimen.

The detailed procedure is explained more readily with the aid of Figure 7. The time pulses locate points A and A' on the load-time and strain-time curves, respectively, and also establish the true period. Points B and B' indicate the point of zero load and, hence, the start of the stress-strain curve. Subsequent increments of time represented by points C-C', D-D', and E-E', are selected. The loads or torques are read off the load cell calibration curve, and the corresponding strains are determined

Figure 7.   Load-Time and Strain-Time Curves
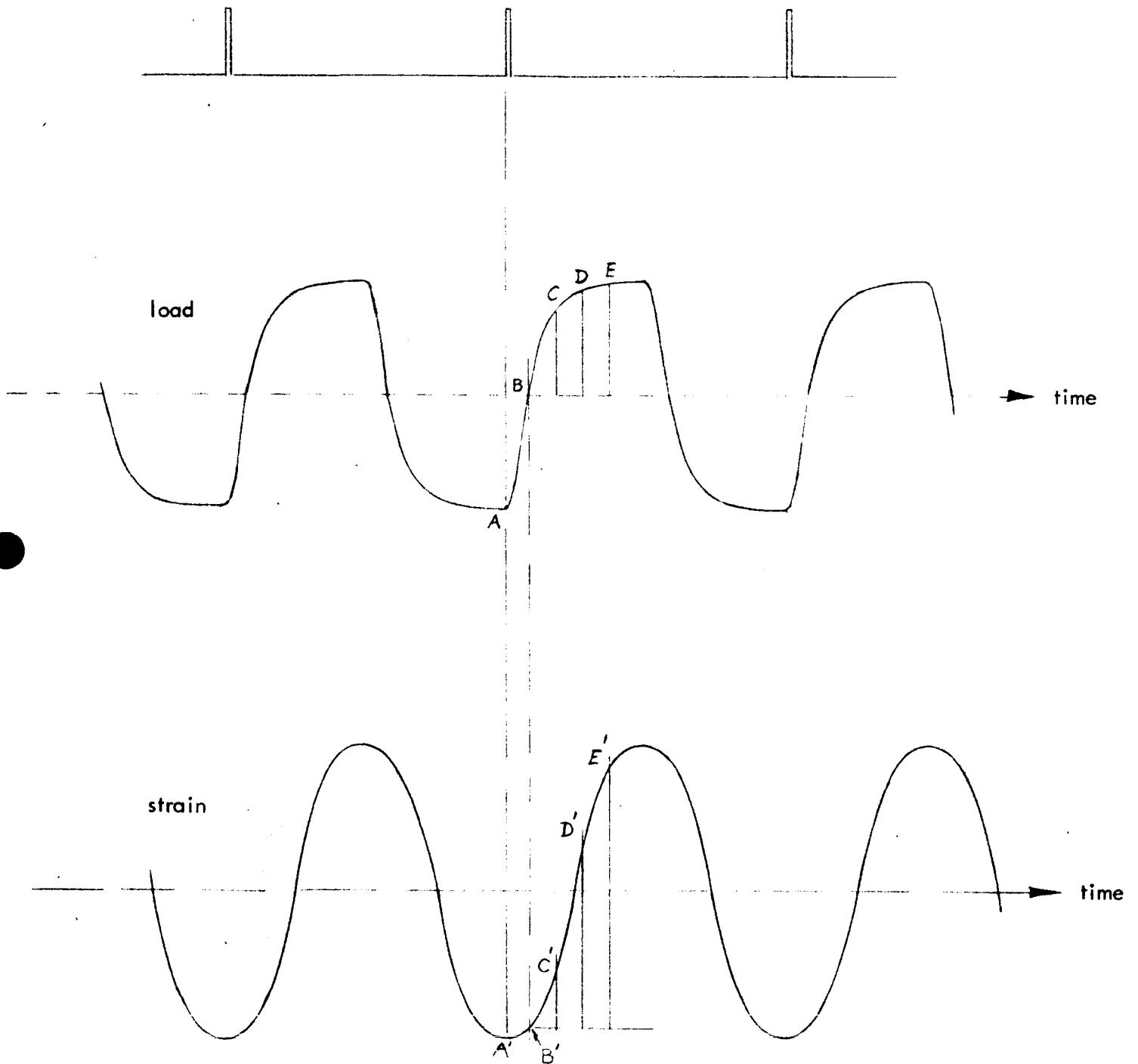
load cell calibration curve, and the corresponding strains are determined from the sinusoidal strain curve, as indicated in the figure, with the amplitude determined from the cam input. Corrections for wind-up in the system are read from the calibration curves using the appropriate torque values and are subtracted from the sinusoidal strains to give the actual strains. Thus, using the dimensions of the thin walled test specimen to convert torque to stress, a stress-strain curve can be plotted.

Preliminary runs have been completed with several 1100-0 aluminum specimens. Some of the data are shown in Table 1 and Figure 8, and a typical stress-strain curve computed by the above procedure is shown in Figure 9.

The fatigue curve of Figure 8 is plotted against plastic shear strain range, which was computed by subtracting both the elastic strain range and the wind-up in the system from the input strain range. The correction for wind-up was small. The solid line has a slope of $-1/2$, corresponding to the empirical relation, $N^{\frac{1}{2}} \Delta \epsilon_p = C$. The value for C for this curve, computed on the basis of the maximum shear criterion, is 0.51. This value compares favorably with similar data in the literature.

Table 1.   Preliminary Data on 1100-0 Aluminum

Sample No.	Total Shear Strain Range	Cycling Frequency (cps)	Cycles to Failure
1	.0128	1.5	2750
2	.0116	17.0	3475
3	.0132	100.0	1380 - 1770
4	.0828	1.5	89
5	.0809	17.0	96
6	.0814	100.0	96
7	.0478	1.5	---
8	.0478	1.5	410
9	.0478	35.0	365

Figure 8.   Fatigue Curve for 1100-0 Aluminum
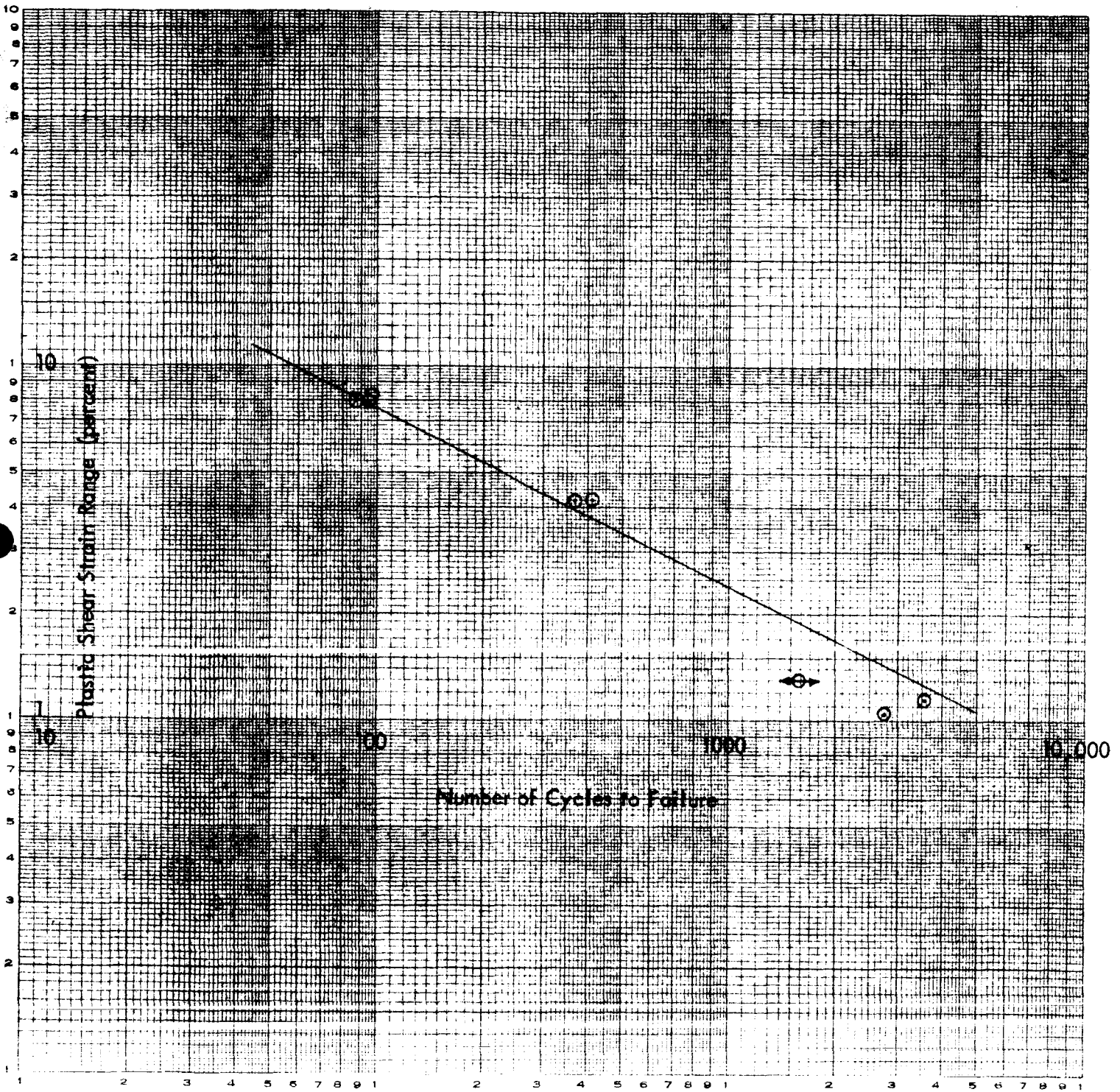
Figure 9.   Cyclic Stress-Strain Curve for 1100-0 Aluminum
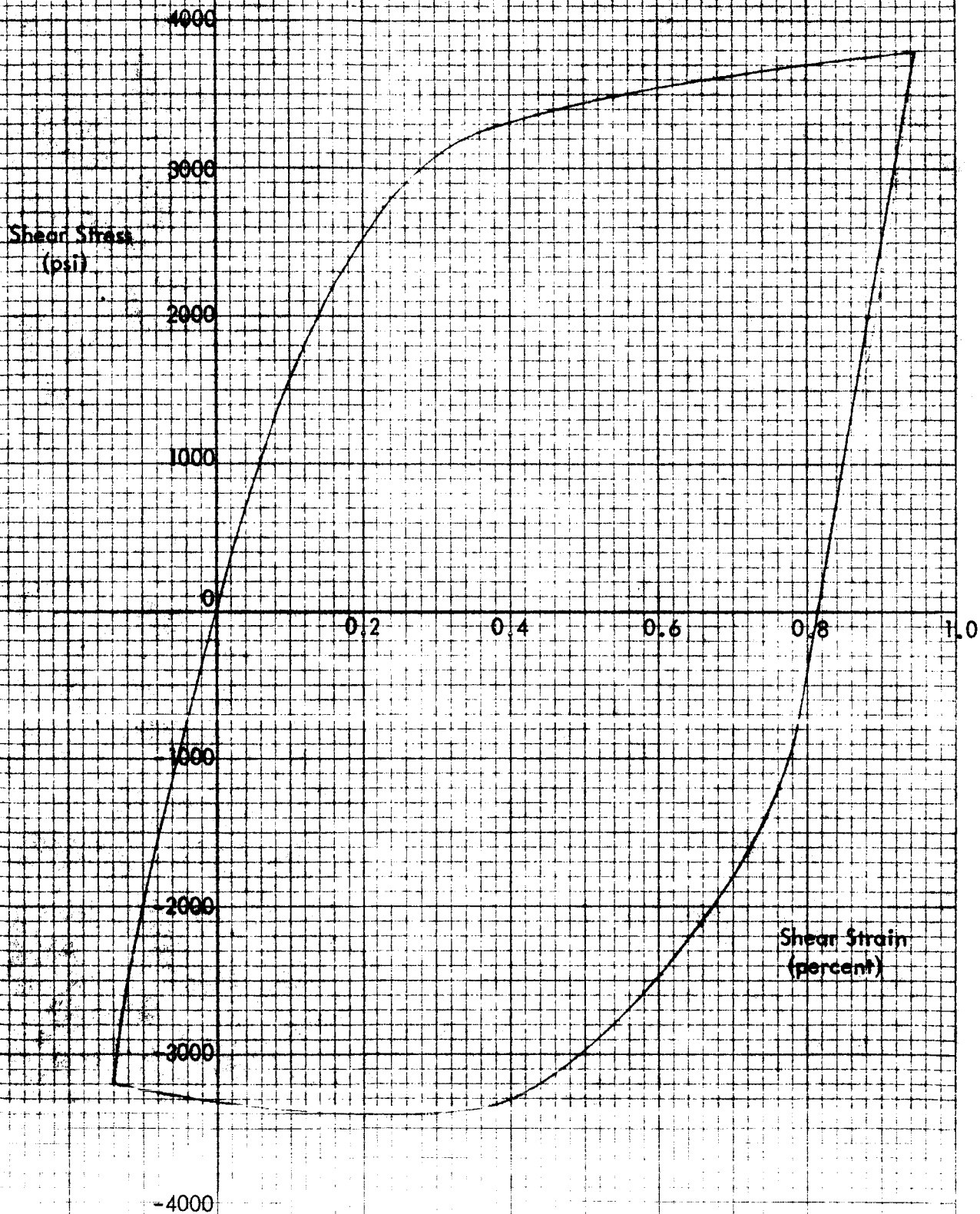
IV. STUDY OF CYCLIC STRAIN ENERGY DEVICES IN RELATION TO CREW PROTECTION APPLICATIONS

Weight limitations and extreme environmental conditions impose severe restrictions on attenuation devices that can be used for crew protection in space vehicles. Further complications arise from the load-stroke limitations imposed by human tolerances, and crew compartment space limitations may require that the available stroke lengths be used at nearly optimum efficiencies. An additional complication arises from the requirement that the devices be capable of recycle operation. For example, a reentry capsule could be subjected to severe decelerations on reentry and, perhaps, multiple impacts on landing due to rolling of the capsule.

Although conventional hydraulic and pneumatic devices might provide the necessary load-stroke and recycle characteristics, they are impractical due to the space environment. "One-shot" destructive mechanisms such as crushing of materials meet the environmental requirements but they cannot effectively meet the load-stroke and recycling requirements. Cyclic strain energy devices, on the other hand, not only satisfy the environmental requirements, but they can be designed to provide the necessary load-stroke and recycle characteristics. In addition, because of their simplicity and their unusually high performance characteristics, these devices can be designed to yield the high reliability required in crew protection systems.

A brief study was undertaken to explore the application of cyclic strain energy devices to crew protection systems. Particular attention was directed to various approaches and mechanisms that might be employed to yield the necessary load-stroke and recycle behavior.

One of the basic requirements for crew protection attenuation devices is that they be capable of prescribed load-stroke behavior. Human tolerances require limitations not only in maximum g-loads but also limitations in onset rates, or maximum rates at which the g-loads can build up. Thus, a prescribed load-stroke curve for a crew protection attenuation device during a single impact might be as indicated ideally in path OABC of Figure 10, where the slope, the maximum load, and the stroke length are specified. If the device is to be used for recycle operation, the subsequent curves might be as indicated by path DEF for reversed loading, or by path DEGH for repeated loading in the same direction. The onset rates and the maximum loads during the subsequent impacts need not be the same as in the initial impact.

Several promising design concepts which can be employed to provide onset rates make use of the "torus" device, which is itself one of the most attractive cyclic strain energy devices investigated thus far. Although this type of device is described in detail in Refs. B and C, a brief description is given in Figure 11. Basically, the device contains a working element which consists of a torus tube or rod, or a section of curved tube or rod. Rolling of the working element during impact, by a mechanism such as one of those shown, produces cyclic tensile and compressive straining of the longitudinal fibers. If it is assumed, for the present discussion, that effects due to work-hardening, rate sensitivity, temperature rise, etc., can be ignored,* then the basic element illustrated

---

*   A discussion of these effects in relation to performance of cyclic strain energy devices is presented in Ref. A, and an experimental evaluation of these effects is currently underway, as described in Sections III and V.
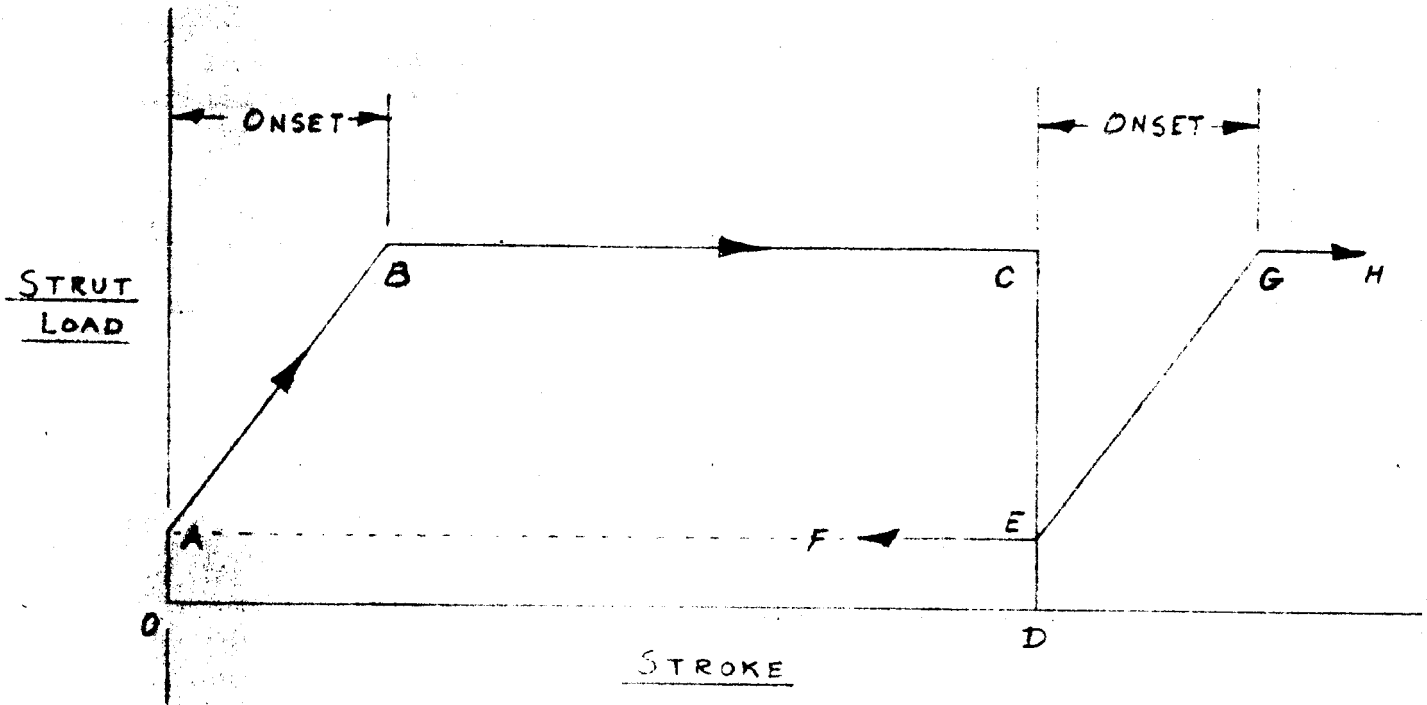
FIG. 10

LOAD - STROKE ... ...

Figure 11.   "Torus" Cyclic Strain Energy Device

A.   Basic working element is a torus tube or rod, or a section of a curved tube or rod.   Rolling of element during impact produces cyclic tensile and compressive straining of longitudinal fibers.

cord

rack and pinion

friction
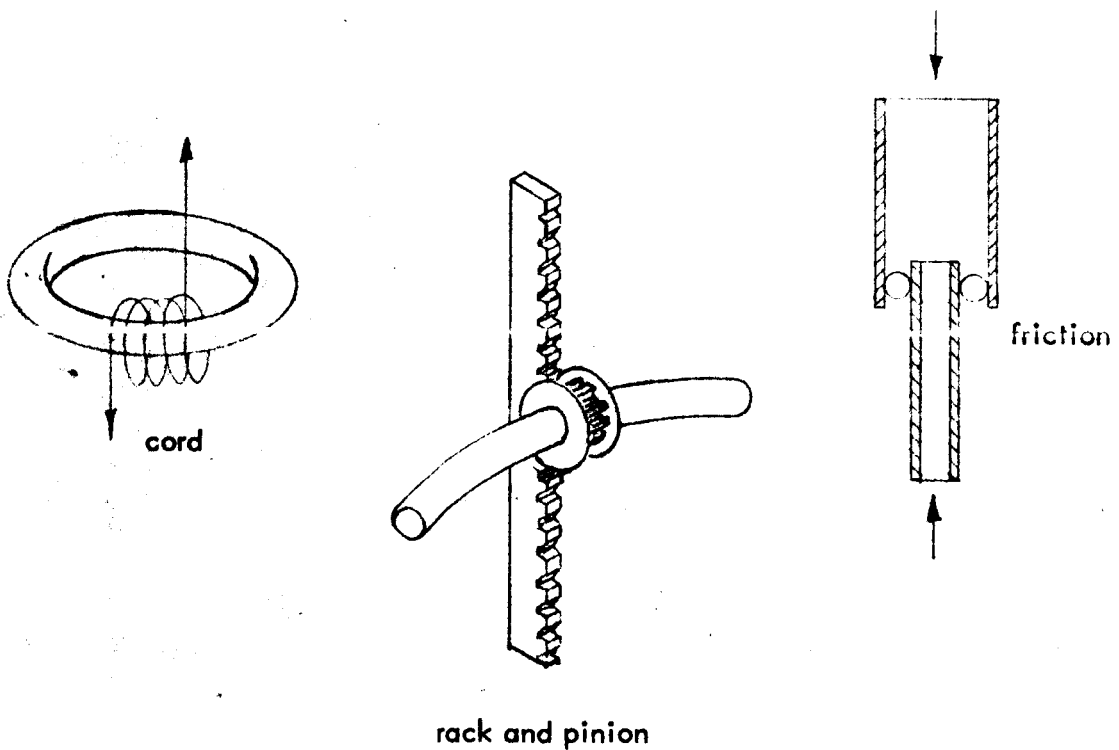
B.   Rolling of working element during impact can be accomplished by various mechanisms, as indicated above.

in Figure 11 may be considered to produce a constant force. In other words, a device which rotates a working element of fixed geometry a fixed number of revolutions per unit stroke length produces essentially a constant resisting force.

It is possible to modify the basic mechanism of Figure 11, or combine two or more mechanisms in such a way as to produce onset rates. Thus, three basic design concepts that can be used to provide onset rates are illustrated in Figure 12. Figure 12a shows a device which progressively engages a cluster of torus elements and thereby yields an onset rate by progressively working more material. Figure 12b illustrates a device which operates on the principle of varying the number of cycles per unit length of stroke. Since the energy absorbed per cycle is constant, a linear variation in number of cycles per unit stroke length yields a linear load-stroke curve. The approach indicated in Figure 12c works on the principle of increasing the plastic strain per cycle and, hence, the energy absorbed per cycle. Thus, if the plastic strain range is increased linearly while the cycles per stroke length remains constant, a linear load-stroke curve results.

The simple torus devices illustrated in Figure 12 provide initial onset rates as well as recycle capability, but the onset rates are very high for subsequent loadings. Also, the maximum load during subsequent loadings is the same as the initial maximum load. More general load-stroke behavior such as indicated in Figure 10 can be achieved with various combinations of devices. For example, the device of Figure 13 illustrates a method of obtaining a path similar to OABCEDEF of Figure 10. A device of this type might suffice in a landing impact application where subsequent impacts were much less severe than the first one.

Outer tube progressively engages torus cluster, thereby working more material with increasing stroke.

(a) Torus Cluster Device

Variable diameter spool
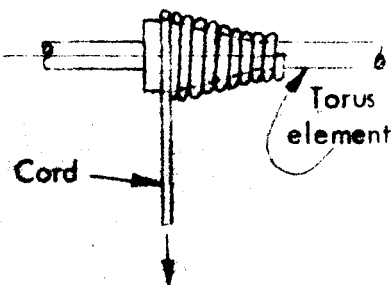
Variable diameter spool increases number of cycles of torus per unit stroke length, thereby increasing energy absorbed per unit stroke length.

(b) Variable Spool Device
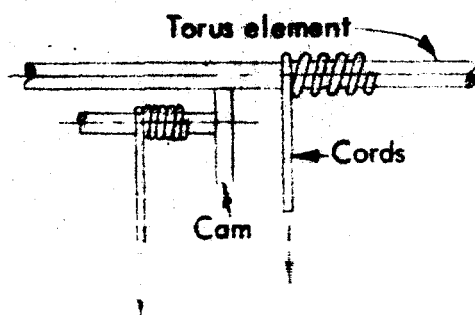
Cords simultaneously roll working metal rod and cam, increasing curvature in rod and plastic strain per cycle.

c) Rotating Cam Device

Figure 12. Torus Devices for Producing Onset Rates

DEFLECTION CAM

VIEW A A

WEDGE RETURN SPRING

CAM ACTUATING WEDGE

A

FRICTION
(CONE)
DEVICE

SPRAGS

CABLE

FIXED STOP
ON WEDGE

ADJUSTABLE
STOP ON
COLUMN

TORUS SECTION

FIG. 13

ENERGY ABSORBING STRUT

This unit resembles a standard shock control strut with pin connections at each end of a telescoping assembly. The assembly consists of a column guided within a housing which contains the entire mechanism to generate the forces and the control units to program the forces during each stroke. The moving column is a square section with a gear rack on two opposite sides and a friction surface on the remaining two sides. Attached at the extreme inside end of the column, a set of inertia sensitive sprags are carried along an endless cable. The cable is run between two pulleys and passes through the wedge friction drive assembly. The pulleys are attached at the opposite ends of the housing to provide a continuous route for the cable. The wedge assembly is driven by the cable between two externally adjustable stops. These stops control the initial force and the limit force of the column. The wedge length and taper determine the onset rate. The wedge deflection is transferred to the torus sections at their external ends by means of opposing cams. The two torus sections are driven by direct gears again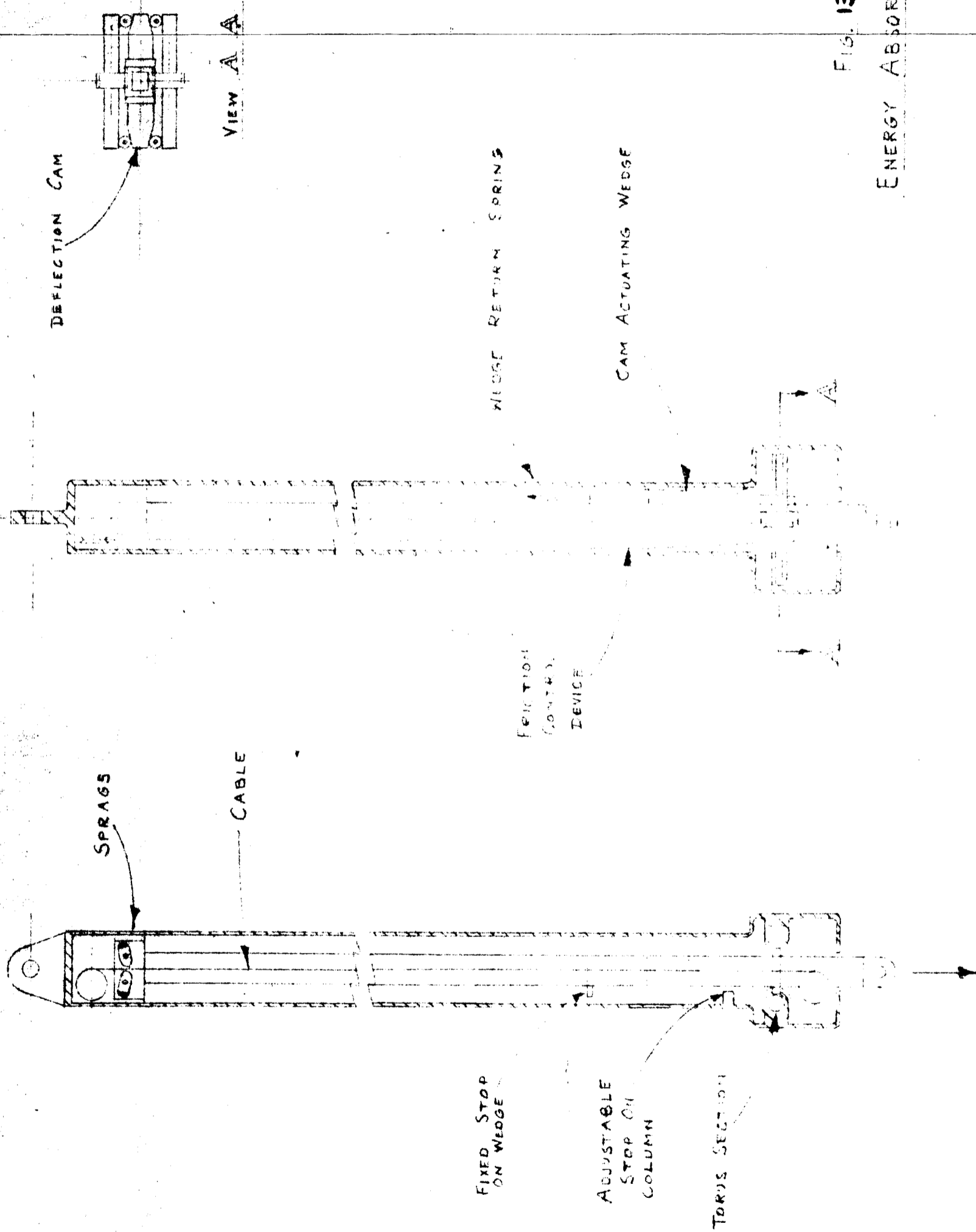st the racks on the column and are in continuous engagement. The housing supports the torus bearings, the drive cams, the column guide bushing, the wedge return springs, and the wedge stops.

The cycle of action of this device can be described by assuming that the suspended body is moving towards ground impact. The initial contact will cause the column to begin to extend outward from the housing and will cause the torus sections to begin rotation at a predetermined resistance due to the initial preset deflection. Immediately upon impact the inertia sensitive sprags at the end of the column will lock against the cable and begin the wedge action against the torus cams. The wedge will move at the same velocity as the column and the torus sections will increase their

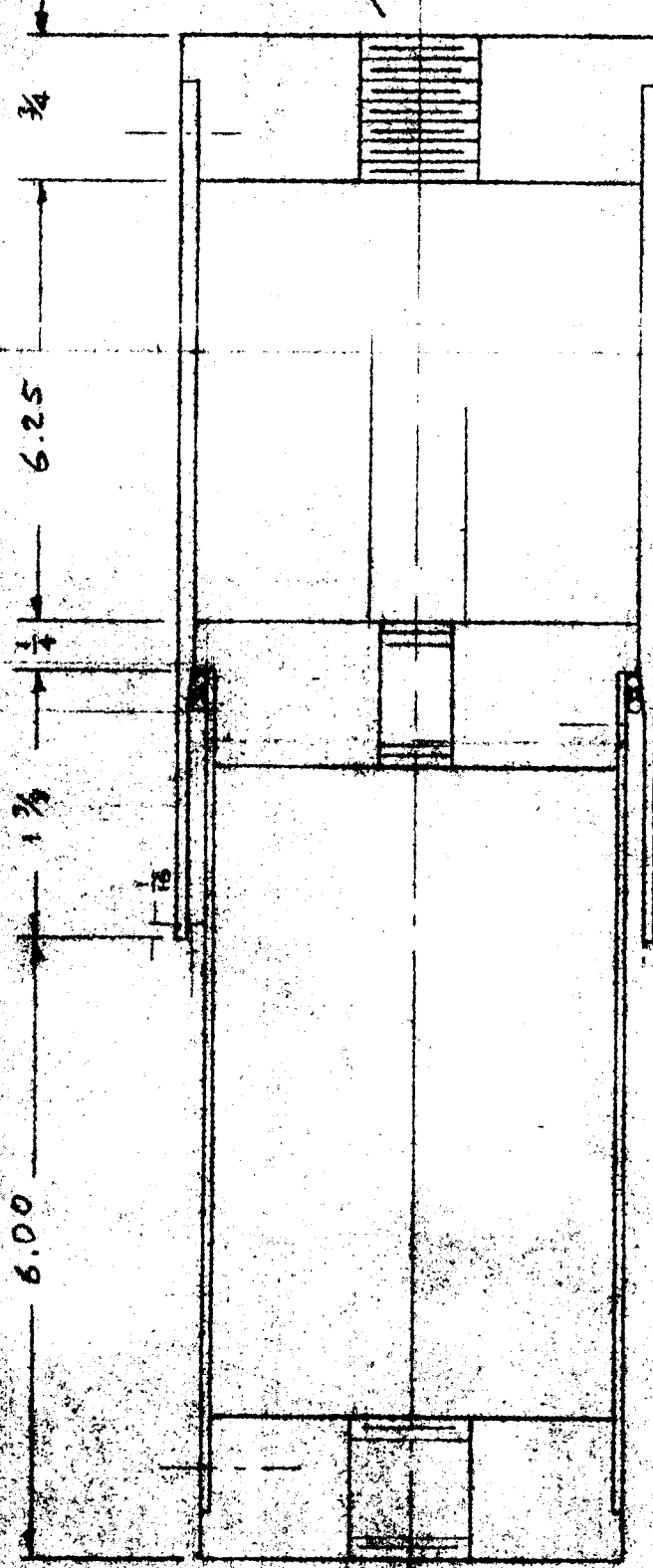resistance in response to the resulting motion until the wedge is halted by the stop. Further motion of the column in the same direction will not increase the torus reaction force. The wedge motion will cause a tension spring unit to become loaded in relation to its deflection in order to provide sufficient force to return the wedge to the initial position at the moment that the impact-caused motion of the column arrives at zero. The inertially actuated sprags will release the cable lock at the moment of zero motion and allow the wedge to return to its original preset position by spring action. Reverse loading of the column will then actuate the torus sections at the original preset force.

It will be possible to alter the preset force at any level from a minimum of a few percent of the maximum to nearly any required amount up to the maximum available. In like manner the maximum force attained at the end of the onset slope may be adjusted at any level between the preset point and the maximum available. In capsule installations such adjustments will be possible while in flight with only a simple calibrated knob. Furthermore, the onset rate could be made adjustable, and within reasonable limits, the entire cycle of forces versus stroke length can be programmed to yield separate onset rates and forces for each repeat stroke of the device.

Several problem areas associated with development of the devices indicated in Figures 12 and 13 can be identified:

A. material behavior (work-hardening, temperature effects, rate effects, etc.)

B. structural and dimensional instability of the working elements

C. driving mechanisms (cord-spool, rack-pinion, friction)

D. problem areas associated with onset and reset mechanisms

5/8 - 18
.578 DRILL

3/4

6.25

1/4

1 3/8

1/8

6.00

DO NOT SCALE DRAWING	
Scale	FULL
Drwn	FAM
Engr	
Appd	PTC
File No.	

Date
9.23.71
8242
Issued

B-1054

The key problem area in a device of this type appears to be that of adequate friction drive. For example, it is important to establish whether or not adequate interference for friction drive can be maintained with practical tolerances. A further question to be answered concerns the effect of dimensional instabilities during cyclic plastic flow of the torus material on the interference and the friction coupling. A preliminary analysis of the friction drive is presented below.

Consider a torus element subjected to a lateral compressive force per unit circumferential length, f_c, due to a particular lateral diametral interference, as shown in Figure 15. If the coefficient of friction is μ, the maximum axial force per unit length of circumference, f, cannot exceed μf_c, i.e.,

$$f \le \mu f_c. \tag{1}$$

The force f is the force per unit circumference which is required to drive the torus, and can be related to the geometric and material properties of the torus, following the analysis of Ref. A.

The work done on the device during stroke dx is related to the area under the hysteresis loop w_p by

$$2\pi \bar{R} f \, dx = (d\nu/dx) \, dx \int w_p \, dV, \tag{2}$$

where $\bar{R}$ is the average major radius of the torus, $d\nu/dx$ is the number of revolutions of the torus per unit stroke length, and V is the volume of working material in the torus. An integral relation is required since in a solid torus element the material is not strained uniformly.

Figure 15.

$$f \le \mu f_c$$

(a)

$$f_c = \overline{\sigma} h$$

$$\frac{\delta_w}{2} = \frac{d}{2} \epsilon$$
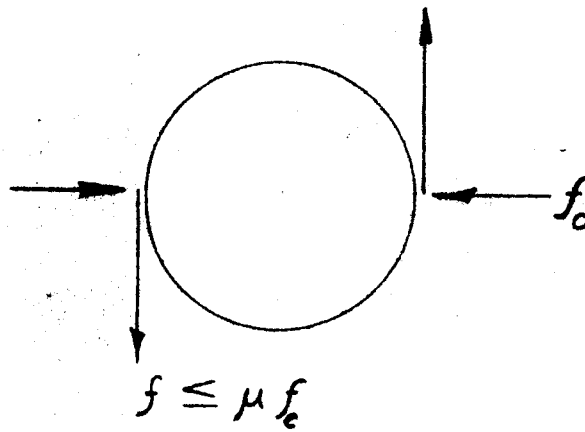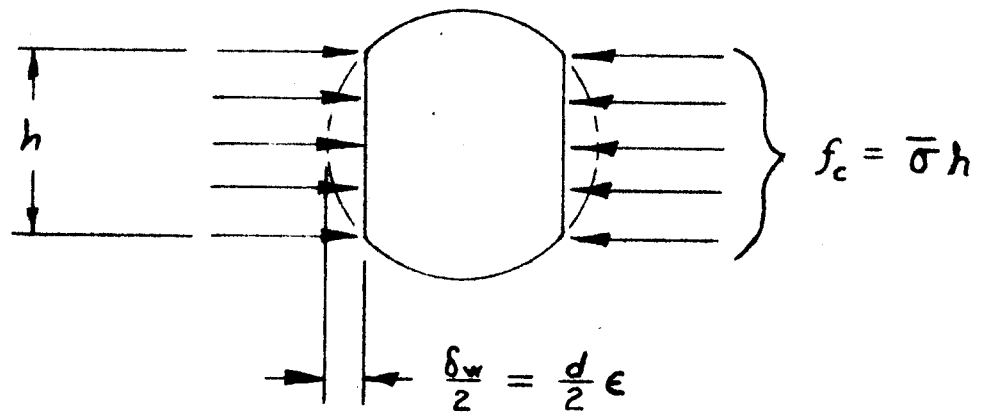
(b)

Lateral Loading and Deformation of Torus Element

For the present friction device, one revolution of the torus corresponds to a stroke of twice the minor circumference of the torus, so that

$$d\mathcal{N}/dx = 1/2 \, \pi \, d, \tag{3}$$

where d is the minor diameter, and Eq. (2) becomes

$$f = (1/4 \pi^2 \bar{R} d) \int_V \omega_p \, dV. \tag{4}$$

With the relations,

$$dV = 4 \pi^2 \bar{R} r \, d r, \tag{5}$$

and

$$\omega_p = \eta \, \Delta \sigma_{max} \, \Delta \epsilon_p , \tag{6}$$

where r is the radial variable for the torus cross-section, $\Delta \sigma_{max}$ and $\Delta \epsilon_p$ are the maximum stress range and plastic strain range, respectively, and η is the ratio of average to maximum stress ranges, Eq. (4) may be written,

$$f = (1/d) \int_0^{d/2} \eta \, \Delta \sigma_{max} \, \Delta \epsilon_p \, r \, d r. \tag{7}$$

Also,

$$\Delta \epsilon_p = \Delta \epsilon_T - (\Delta \sigma_{max}/E), \tag{8}$$

where $\Delta \epsilon_T$ is the total strain range and E is Young's modulus. If the minor diameter

of the torus is small compared with the major diameter (i.e., wire thickness small compared with tube diameter), then the approximate relation exists,

$$\Delta \epsilon_T = 2r/\bar{R}.$$ (9)

If it is also assumed that the elastic strain range is negligible, and if $\gamma \Delta \sigma_{max}$ is replaced by the average stress range $\overline{\Delta \sigma}$, Eqs. (7) to (9) can be combined to give

$$f = (2/d\bar{R}) \int_0^{d/2} \overline{\Delta \sigma} \, r^2 \, dr.$$ (10)

With the further assumption that $\overline{\Delta \sigma}$ is independent of strain range, Eq. (10) can be integrated to yield the design relation,

$$f = (1/12)(d^2/\bar{R}) \overline{\Delta \sigma}.$$ (11)

Another relation between the compressive force f_c and the diametral interference δ is required. This interference results in "hoop" expansion and compression of the outer and inner tubes, respectively, and in lateral compression or flattening of the torus wire. It is desirable to limit both the hoop deformation of the tubes as well as the compression of the wire to the elastic range, if possible. A rigorous treatment of the contact problem to determine the elastic deformation of the torus wire is quite complex. However, an approximate treatment of the plastic deformation problem is possible, and may prove adequate for design purposes.

Let δ_w and δ_T be the diametral interference that goes into deformation of the wire and hoop deformation of the tubes, respectively, so that

$$\delta = \delta_w + \delta_T . \tag{12}$$

If it is assumed that the wire is flattened well into the plastic range, as indicated in Figure 15b, a relation can be obtained between δ_w and f_c. Thus, from the figure,

$$\delta_w = d \epsilon , \tag{13}$$

where ϵ is the maximum diametral compressive strain, and

$$f_c = \overline{\sigma} h , \tag{14}$$

where $\overline{\sigma}$ is an average compressive stress, and h is the width of the flattened section. From geometrical considerations,

$$h = d \sqrt{2\epsilon} , \tag{15}$$

so that, with Eqs. (13) and (14),

$$\delta_w = f_c^2 / 2 d \overline{\sigma}^2 . \tag{16}$$

From simple hoop stress relations,

$$\delta_T = p R_o^2 / t_o E_o + p R_I^2 / t_I E_I = p (R_o^2 / t_o E_o + R_I^2 / t_I E_I) , \tag{17}$$

where p is the effective pressure* exerted by the torus elements on the tube, E_o and

---

* Simple hoop relations are applicable provided the torus cluster is of sufficient length. For a single torus exerting a line load more complicated relations would be required.

-32-

E_I are Young's moduli for the tubes, R_o and R_I are the average radii of the outer and inner tubes, and t_o and t_I are their respective thicknesses. For a torus cluster of sufficient length the pressure p is given by

$$p = n f_c \qquad (18)$$

where n is the number of torus elements per unit axial length. With this relation, Eq. (17) becomes

$$\delta_T = n f_c \, (R_o^2/t_o E_o + R_I^2/t_I E_I). \qquad (19)$$

The hoop stresses in the tubes can be calculated from

$$\sigma_o = R_o \, \delta_T / \left[t_o \, (R_o^2/E_o t_o + R_I^2/E_I t_I) \right],$$

$$\sigma_I = R_I \, \delta_T / \left[t_I \, (R_o^2/E_o t_o + R_I^2/E_I t_I) \right], \qquad (20)$$

and Eq. (13) gives the maximum lateral compressive strain in the wire for a given value of δ_w.

For the test device of Figure 14, the torus wire is 1100-0 aluminum 0.064 inch in diameter, the outer tube is 6061 T6 aluminum alloy with a 2.50 inch O.D. and 0.070 inch wall, and the inner tube is 2024 T3 aluminum alloy with a 2.24 inch O.D. and a 0.076 inch wall. Thus, taking $E_o = 10 \times 10^6$ psi and $E_I = 10.6 \times 10^6$ psi, Eqs. (20) give

$$\sigma_o = 4.87 \times 10^6 \, \delta_T \quad \#/in^3, \qquad \sigma_I = 3.97 \times 10^6 \, \delta_T \quad \#/in^3 \qquad (21)$$

Assuming the maximum number of torus elements possible per unit axial length, $n = 1/d$, and Eq. (19) gives the relation

$$\delta_T = 5.60 \times 10^{-5} \, f_c \quad in^2/\# . \qquad (22)$$

Eqs. (21) and (22) provide simple numerical relations for the compressive force and hoop stresses in the tubes as a function of δ_T. Similarly, using $\overline{\sigma} = 5,000$ psi for the 1100-0 aluminum torus element, Eq. (16) gives

$$\delta_w = 3.12 \times 10^{-7} \, f_c^2 \quad in^3/\#^2 . \qquad (24)$$

Taking a yield stress for the outer tube of 40,000 psi, the maximum allowable value for δ_T is, from the first of Eqs. (21), 0.0082 inch. Using this value in Eq. (22), the maximum allowable value for f_c is 146 $\#/in$. Also, from Eq. (24), the maximum value for δ_w is 0.00675 inch, corresponding to a lateral compressive strain in the wire of 0.106. It appears that this magnitude of compressive strain would be prohibitive for a successful drive. Consequently, it is of interest to determine the minimum inter- ference that would be required to drive the torus element, based on Eqs. (1) and (11). For this purpose, however, a value of $\overline{\Delta\sigma}$ for the cyclically strain-hardened material is used. Thus, taking $\overline{\Delta\sigma} = 20,000$ psi, Eq. (11) gives a value of 5.94 $\#/in$ for f. Using this value with $\mu = 0.5$, the minimum value for f_c is 11.8 $\#/in$, which corresponds to $\delta_T = 6.60 \times 10^{-4}$ in, $\delta_w = 4.35 \times 10^{-5}$ in and a lateral com- pressive strain in the wire of 6.79×10^{-4}. These results are shown in Figure 16.

Figure 16. Hoop Deformation of Tubes and Lateral Compression of Torus Element vs. Lateral Compressive Force
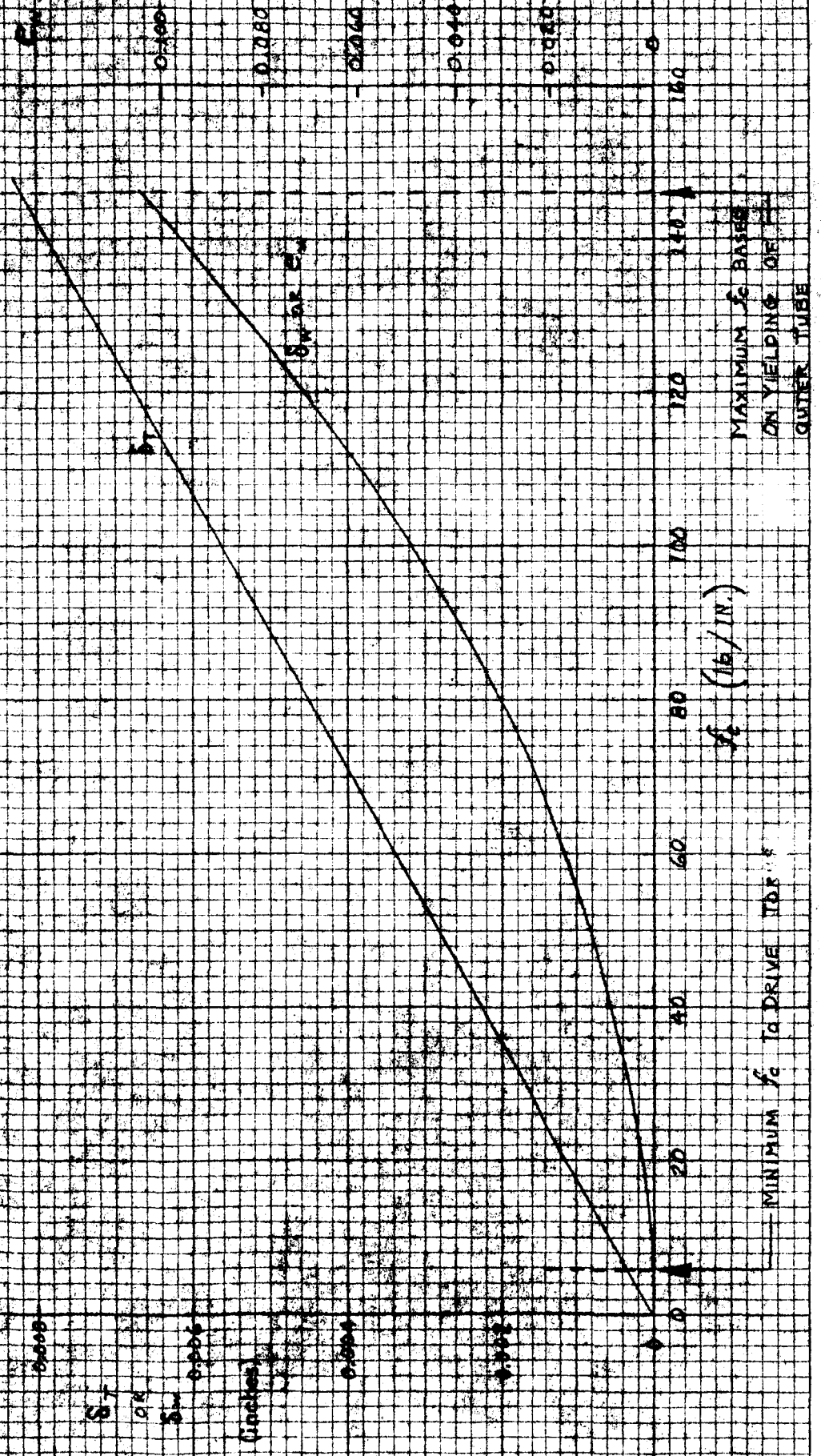
This numerical example illustrates an interesting feature with regard to devices of this type. For column tubes and working elements of practical dimensions there exists considerable elasticity from hoop deformation of the tubes. This elasticity insures an adequate compressive force to drive the elements which is maintained over a significant range of tolerances. Thus, for the test device, diametral interferences from 0.0007 inch to 0.0090 inch provide sufficient lateral force on the elements without exceeding the yield strength of the tubes. However, the larger interferences may result in too much lateral compressive strain in the torus element for this particular design. Thus, the permissible range of interferences could be increased by selecting tubes with smaller wall thicknesses and, hence, greater flexibility.

The flexibility in the column tubes makes it possible to adjust the resisting force in the column and produce onset rates by utilizing more than one material as well as more than one element. It further simplifies the design of the device and alleviates, somewhat, the problem of dimensional instability of the working element.

The foregoing design analysis was based on the assumption of uniform hoop deformation in the column tubes, i.e., a torus cluster of sufficient axial length. For the case of fewer torus elements the hoop relations can be obtained from the results of a radial line load applied to a circular cylinder.

V.   FUTURE WORK

During the next quarterly period emphasis will be placed on the following areas:

A.   Completion of the cyclic torsional testing of the aluminum, stainless steel, and molybdenum specimens

B.   Evaluation of the test results in terms of flow and fatigue behavior, and correlation of the data with similar results reported in the literature for lower rates of straining

C.   Fabrication and testing of the friction drive torus impact device described in the present report, and correlation of the test data with the analytical models developed under this contract

D.   Study of viscoelastic behavior of non-metals in relation to cyclic strain energy devices, and selection of promising non-metals to be evaluated under a future phase of the experimental program.

REFERENCES

A.   Platus, David L., Patrick J. Cunningham, and Frank A. Marovich.   First Quarterly Progress Report on "Concepts of Multiple-Impact Study of Energy Absorption, ARA Report #23, 1 July 1963.

B.   Platus, David L., and Frank A. Marovich.   An Invention for Multiple-Impact High Energy Absorbing Devices Utilizing Cyclic Deformation of Metals, ARA Report #9, 18 December 1962.

C.   Platus, David L.   A Reduction to Practice of a Multiple-Impact High Energy Absorbing Device Utilizing Cyclic Deformation of a Metal, ARA Report #16, 30 March 1963.